# Growth and Structure of Surface-Initiated Poly(*n*-alkylnorbornene) Films

Brad J. Berron, Evan P. Graybill, and G. Kane Jennings*

*Department of Chemical Engineering, Vanderbilt University, Nashville, Tennessee 37235*

*Received June 15, 2007. In Final Form: August 7, 2007*

We report the surface-initiated growth of poly(alkylnorbornene) films via ring-opening metathesis polymerization (ROMP). The films are grown by exposure of a vinyl-terminated self-assembled monolayer (SAM) on gold to Grubbs first-generation catalyst and the subsequent exposure to an alkylnorbornene monomer. We investigate the influence of alkyl side chains on the structure, barrier, surface properties, and the growth kinetics of surface-initiated ROMP-type poly(norbornene) films. Rate constants for film growth are estimated for the comparison of monomer reactivity. The rate constant for film growth decreases by 3 orders of magnitude from norbornene to decylnorbornene, indicating a strong effect of chain length on initiation and/or propagation rates. Reflectance−absorption infrared spectroscopy is used to show the molecular level packing within the poly(alkylnorbornene) films is disrupted by the alkyl side chains. Tapping-mode atomic force microscopy is used to show that norbornene, butylnorbornene, and hexylnorbornene polymerize from the surface to form dense coatings, whereas decylnorbornene polymerizes to form isolated polymer clusters. The methyl terminus of the alkyl side chains increases the hydrophobicity of the poly(alkylnorbornene) films ($\theta_A(H_2O) = 109-114°$) beyond that of a typical poly(norbornene) film ($\theta_A(H_2O) \sim 106°$). The additional hydrophobicity throughout the film correlates with superior resistances against redox probes ($R_f \sim 10^5\ \Omega\cdot cm^2$) for poly(hexylnorbornene) when compared to polynorbornene ($R_f \sim 10^4\ \Omega\cdot cm^2$). The resistance of the poly(decylnorbornene) film ($R_f \sim 10^2\ \Omega\cdot cm^2$) is consistent with its nonuniform, cluster-like morphology.

## Introduction

Surface-initiated polymerizations refer to the continual addition of repeat units at the termini of surface-tethered chains and offer several advantages over traditional coating methods, including rapid processing,[1] improved adhesion due to a chemical coupling of the initiator/polymer chain to the substrate, the ability to prepare uniform, conformal coatings on objects of any shape,[2,3] excellent control over film thickness,[1−4] tunable grafting densities,[5] and good control over depth-dependent composition.[6−8] These films are of potential use in applications traditionally dominated by spin coating and solution casting, such as polymer dielectric layers,[1] etch resists for lithography,[9,10] responsive polymer films,[11,12] and membrane separations.[13,14] The ability to grow films with new compositions, architectures, and properties could have a profound impact on these applications.

We report the development of a surface-initiated polymer film composed of poly(*n*-alkylnorbornene)s. Our approach (Figure 1) begins by preparing a vinyl-terminated monolayer on a gold substrate via exposure to allyl mercaptan. The terminal vinyl group is then reacted with a metathesis catalyst, immobilizing the catalyst on the substrate. The bound catalyst is then reacted with the desired monomer through ring-opening metathesis polymerization (ROMP) to create a surface-tethered poly(*n*-alkylnorbornene) film. This article reports the first surface-initiated growth of poly(*n*-alkylnorbornene) films as well as the first use of allyl mercaptan as a linkage between a substrate and a metathesis catalyst. Allyl mercaptan is a convenient choice, as it is inexpensive and commercially available. Previously reported thiol-based linking molecules all have been custom synthesized for the particular application.

Ring-opening metathesis polymerizations exhibit rapid kinetics under mild conditions, producing among the thickest surface-initiated films ever produced when norbornene is used as the monomer (>1 $\mu$m).[1,4,15−17] Typical surface-initiated ROMP experiments are run for short time periods (<60 min) at room temperature. The predominate ROMP monomers studied in surface-initiated cases have been norbornene and its functional derivatives,[1,4,5,15−18] due to the high reactivity of norbornene in ROMP and the ease of functionalized monomer synthesis.[19]

Functional derivatives of norbornene can polymerize to produce films with wide-ranging properties and applications, including functionalization of chromatographic supports[15,20] to improve

* To whom correspondence should be addressed. E-mail: kane.g.jennings@vanderbilt.edu. Tel.: (615) 322-2707. Fax: (615) 343-7951.

(1) Rutenberg, I. M.; Scherman, O. A.; Grubbs, R. H.; Jiang, W.; Garfunkel, E.; Bao, Z. *J. Am. Chem. Soc.* **2004**, *126*, 4062−4063.
(2) Jennings, G. K.; Brantley, E. L. *Adv. Mater.* **2004**, *16*, 1983−1994.
(3) Buchmeiser, M. R. In *Surface-Initiated Polymerization I*, Springer: Berlin, 2006; Vol. 197, pp 137−171.
(4) Kim, N. Y.; Jeon, N. L.; Choi, I. S.; Takami, S.; Harada, Y.; Finnie, K. R.; Girolami, G. S.; Nuzzo, R. G.; Whitesides, G. M.; Laibinis, P. E. *Macromolecules* **2000**, *33*, 2793−2795.
(5) Jordi, M. A.; Seery, T. A. P. *J. Am. Chem. Soc.* **2005**, *127*, 4416−4422.
(6) Matyjaszewski, K.; Miller, P. J.; Shukla, N.; Immaraporn, B.; Gelman, A.; Luokala, B. B.; Siclovan, T. M.; Kickelbick, G.; Vallant, T.; Hoffmann, H.; Pakula, T. *Macromolecules* **1999**, *32*, 8716−8724.
(7) Boyes, S. G.; Brittain, W. J.; Weng, X.; Cheng, S. Z. D. *Macromolecules* **2002**, *35*, 4960−4967.
(8) Kim, J.-B.; Huang, W.; Bruening, M. L.; Baker, G. L. *Macromolecules* **2002**, *35*, 5410−5416.
(9) Zhou, F.; Liu, W. M.; Hao, J. C.; Xu, T.; Chen, M.; Xue, Q. J. *Adv. Funct. Mater.* **2003**, *13*, 938−942.
(10) Husemann, M.; Mecerreyes, D.; Hawker, C. J.; Hedrick, J. L.; Shah, R.; Abbott, N. L. *Angew. Chem., Int. Ed.* **1999**, *38*, 647−649.
(11) Bai, D. S.; Habersberger, B. M.; Jennings, G. K. *J. Am. Chem. Soc.* **2005**, *127*, 16486−16493.
(12) Ayres, N.; Boyes, S. G.; Brittain, W. J. *Langmuir* **2007**, *23*, 182−189.
(13) Balachandra, A. M.; Baker, G. L.; Bruening, M. L. *J. Membr. Sci.* **2003**, *227*, 1−14.
(14) Bai, D. S.; Elliott, S. M.; Jennings, G. K. *Chem. Mater.* **2006**, *18*, 5167−5169.
(15) Buchmeiser, M. R.; Sinner, F.; Mupa, M.; Wurst, K. *Macromolecules* **2000**, *33*, 32−39.
(16) Weck, M.; Jackiw, J. J.; Rossi, R. R.; Weiss, P. S.; Grubbs, R. H. *J. Am. Chem. Soc.* **1999**, *121*, 4088−4089.
(17) Liu, X. G.; Guo, S. W.; Mirkin, C. A. *Angew. Chem., Int. Ed.* **2003**, *42*, 4785−4789.
(18) Li, X. M.; Huskens, J.; Reinhoudt, D. N. *Nanotechnology* **2003**, *14*, 1064−1070.

10.1021/la7017902 CCC: $37.00 
Published on Web 10/11/2007

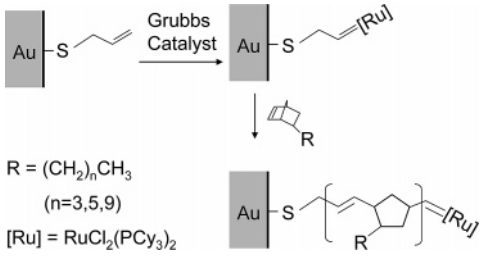


**Figure 1.** Schematic illustration of the gold surface preparation by attachment of allyl mercaptan, attachment of Grubbs' catalyst, and the ring-opening metathesis polymerization (ROMP) of alkylnorbornenes.

selectivity and modification of carbon nanotubes to improve dispersability in common solvents.[2] The conservation of the olefin functionality in these films provides an opportunity for further functionalization, which may lead to a wide variety of end uses for this family of films. Boyd and Schrock have demonstrated facile sulfonation and epoxidation of modified polynorbornenes.[21] A sulfonated thin film could be useful in proton/ion/water transport applications,[22] whereas an epoxide is a useful intermediate for further film functionalization including conversion to an alcohol.[21] For traditional barrier films, hydrogenation would be useful in preventing unwanted side reactions.[23,24] While surface-initiated poly(alkylnorbornene) films have yet to be reported, Hatjopoulos and Register[23] recently published a study on the bulk elastomeric properties of ROMP-type poly(alkylnorbornene)s and their hydrogenated derivatives. They observed a decrease in glass transition temperature ($T_g$) with increasing alkyl chain length, which was attributed to the alkyl side chains of the polymer acting as plasticizers to disrupt packing within the polymer.

Previous studies have shown the polymerization kinetics of substituted norbornene monomers to be slower than that of norbornene.[23,25,26] The polymerization kinetics of *n*-alkylnorbornenes in solution using a Schrock-type catalyst was studied by Hatjopoulos and Register.[23] They reported a moderate decrease in the polymerization rate constant as the length of the alkyl side chain increased. The kinetic penalty associated with the alkyl side chain may be exaggerated on a surface due to steric hindrances associated with a solid support.

Here, we investigate the effect of alkyl chain length on the kinetics of surface-initiated polymerization of alkylnorbornenes. We use a series of poly(alkylnorbornene) films of comparable thickness to evaluate the dependence of film structure, as well as surface and barrier properties, on alkyl side-chain length. Surface-initiated poly(alkylnorbornene) films should have a low surface energy, due to a surface composed of both methyl and methylene functionality. Surface-initiated ROMP has been shown to grow uniform coatings given appropriate monomers and reaction conditions.[1,4,17,27,28] We use atomic force microscopy (AFM) to investigate the uniformity and morphology of the surface-initiated poly(alkylnorbornene) films and electrochemical impedance spectroscopy (EIS) to measure the barrier properties of the films. The barrier properties of hydrocarbon-based surface-initiated films have been extensively studied and show excellent resistance to water and ion transport.[29−32] The barrier properties of some poly(alkylnorbornene) films should prove to have comparable film resistances to dense hydrocarbon-based surface-initiated films, making them suitable for numerous applications as surface coatings.

## Experimental Section

**Materials.** 5-*n*-Butylnorbornene (98%), 5-*n*-hexylnorbornene (98%), and 5-*n*-decylnorbornene (98%) monomers were provided by Promerus Electronic Materials and used as received. Grubbs' first generation catalyst (benzylidene-bis(tricyclohexylphosphine)-dichlororuthenium), 1-dodecanethiol (98%), 2-propene-1-thiol (allyl mercaptan, 70%), $K_3Fe(CN)_6$ (99%), and $K_4Fe(CN)_6 \cdot 3H_2O$ (99%) were used as received from Sigma-Aldrich. Norbornene (NB, 99%) was used as received from MP Biomedicals. Dichloromethane (99.9%) and toluene (99.9%) were used as received from Fisher Scientific. Gold shot (99.99%) and chromium-coated tungsten filaments were obtained J&J Materials and R.D. Mathis, respectively. Silicon wafers (100) were obtained from Montco Silicon. Ethanol (absolute) was used as received from AAPER. Deionized water (16.7 MΩ·cm) was purified with a Modu-Pure system.

**Preparation of Gold Substrates.** Silicon wafers were rinsed with ethanol and water, then dried in a nitrogen stream. Chromium (100 Å) and gold (1250 Å) were sequentially evaporated onto the silicon wafers at rates of $<2$ Å $s^{-1}$ in a diffusion-pumped chamber with a base pressure of $4 \times 10^{-6}$ torr. The wafers were typically cut into sample sizes of 1.5 cm × 3.5 cm.

**Polymerization.** Gold substrates were placed in a 2.0 mM ethanolic solution of allyl mercaptan for 30 min. The initiator-coated substrates were exposed to a 5 mM solution of Grubbs catalyst in dichloromethane for 15 min. The catalyst-coated films were rinsed with dichloromethane and immediately placed in a monomer solution containing either 0.27 M norbornene, 0.50 M butylnorbornene, or 1.89 M hexylnorbornene in dichloromethane for 15 min to achieve ∼45 nm polymer films. Poly(decylnorbornene) films were analogously prepared with a 3.0 M solution of decylnorbornene in dichloromethane to yield ∼10 nm polymer films. The films were sequentially rinsed with dichloromethane, ethanol, and water and dried in a nitrogen stream. Catalyst-coated films were immersed in 1.0 M monomer solutions for 10 s and 2, 15, and 60 min for the determination of kinetic rate constants. Samples for kinetic studies were also sonicated in dichloromethane for 2 min after polymerization to remove any unbound material.

**Characterization Methods.** Film properties were evaluated using the following methods to determine the structure and properties of the films. Reflectance−absorption infrared spectroscopy (RAIRS) was performed using a Varian 3100 FT-IR spectrometer in single-reflection mode with a universal sampling accessory and a liquid nitrogen cooled, narrow-band MCT detector. p-Polarized light was incident at 80° from the surface normal. Spectra were collected using 200 scans at a resolution of 2 $cm^{-1}$ using a clean gold sample as a reference. Film coverage and surface morphology were investigated with a Digital Instruments MultiMode Nanoscope IIIa (AFM). Height contrast images (25 $\mu$m × 25 $\mu$m) were collected in tapping mode with a silicon tip. Ellipsometric thicknesses were determined from a J.A. Woollam M-2000DI variable angle spectroscopic ellipsometer. Thicknesses and refractive indices were fit to data taken at 75° from the surface normal over wavelengths from 400 to 700 nm. Optical constants of the underlying gold used in the preparation of each sample were taken prior to polymer film

(19) Pasquale, A. J.; Fornof, A. R.; Long, T. E. *Macromol. Chem. Phys.* **2004**, *205*, 621−627.
(20) Buchmeiser, M. R. *Macromol. Rapid Commun.* **2001**, *22*, 1082−1094.
(21) Boyd, T. J.; Schrock, R. R. *Macromolecules* **1999**, *32*, 6608−6618.
(22) Iojoiu, C.; Marechal, M.; Chabert, F.; Sanchez, J. Y. *Fuel Cells* **2005**, *5*, 344−354.
(23) Hatjopoulos, J. D.; Register, R. A. *Macromolecules* **2005**, *38*, 10320−10322.
(24) Lee, L. B. W.; Register, R. A. *Macromolecules* **2005**, *38*, 1216−1222.
(25) Seehof, N.; Grutke, S.; Risse, W. *Macromolecules* **1993**, *26*, 695−700.
(26) Feast, W. J.; Gimeno, M.; Khosravi, E. *J. Mol. Catal. A: Chem.* **2004**, *213*, 9−14.
(27) Harada, Y.; Girolami, G. S.; Nuzzo, R. G. *Langmuir* **2003**, *19*, 5104−5114.
(28) Juang, A.; Scherman, O. A.; Grubbs, R. H.; Lewis, N. S. *Langmuir* **2001**, *17*, 1321−1323.
(29) Guo, W.; Jennings, G. K. *Adv. Mater.* **2003**, *15*, 588−591.
(30) Brantley, E. L.; Holmes, T. C.; Jennings, G. K. *J. Phys. Chem. B* **2004**, *108*, 16077−16084.
(31) Bantz, M. R.; Brantley, E. L.; Weinstein, R. D.; Moriarty, J.; Jennings, G. K. *J. Phys. Chem. B* **2004**, *108*, 9787−9794.
(32) Brantley, E. L.; Holmes, T. C.; Jennings, G. K. *Macromolecules* **2005**, *38*, 9730−9734.

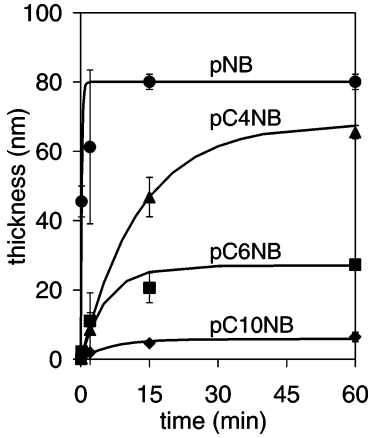


**Figure 2.** Ellipsometric film thickness of poly(alkylnorbornene) films grown from 1.0 M alkylnorbornene solutions in dichloromethane for the indicated times. Solid curves represent fits of the data using eq 3.

deposition and used as a baseline for thickness measurements. Reported thickness values and errors represent the averages and standard deviations, respectively, from at least six independently prepared samples.

Contact angles of water and hexadecane were measured with a Rame−Hart manual contact angle goniometer. Advancing and receding contact angle measurements were taken on both sides of ~5 $\mu$L drops of both water and hexadecane with the microliter syringe tip remaining inside the drop during measurement. Reported values and errors represent the averages and standard deviations, respectively, from at least six independently prepared samples.

Electrochemical impedance spectroscopy was performed with a Gamry Instruments CMS300 impedance system interfaced to a personal computer. A flat cell (EG&G) was used to selectively expose 1.0 $cm^2$ of each sample as the working electrode to an aqueous solution of 1 mM $K_3Fe(CN)_6$, 1 mM $K_4Fe(CN)_6 \cdot 3H_2O$, and 0.1 M $Na_2SO_4$. Measurements were taken using a Ag/AgCl/saturated KCl reference electrode with evaporated gold on silicon as the counter electrode. Data were collected between $10^{-1}$ and $10^4$ Hz and fit using a Randles equivalent circuit to determine resistance and capacitance values. Reported values and errors represent the averages and standard deviations, respectively, from at least eight independently prepared samples.

## Results and Discussion

**Growth Kinetics.** We investigated the kinetics of film growth by exposure of the ROMP-active monolayers to 1.0 M alkylnorbornene solutions for 10 s and 2, 15, and 60 min, followed by measuring the thicknesses of the resulting films. Figure 2 shows the experimental thickness for films grown from norbornene (NB), butylnorbornene (C4NB), hexylnorbornene (C6NB), and decylnorbornene (C10NB) monomers. At short times, the active chains grow and the thickness of the poly(alkylnorbornene) film increases rapidly with time. As the catalyst deactivates, the growth of the poly(alkylnorbornene) chains ceases and the film thickness approaches a constant value that decreases as the side-chain length is increased.

The description of ROMP kinetics necessitates the determination of initiation, polymerization, and termination kinetic rate constants. As a tool to estimate the *relative* kinetics of film growth for this series of alkylnorbornenes, we begin with a simplified kinetic model set forth by Harada et al.,[27] which assumes an initial chain density. The time dependence of film thickness ($d$) was given as

$$d = \left(\frac{k_p M}{k_t}\right)\left(\frac{m_o P_I}{\rho}\right)(1 - e^{-k_t t}) \quad (1)$$

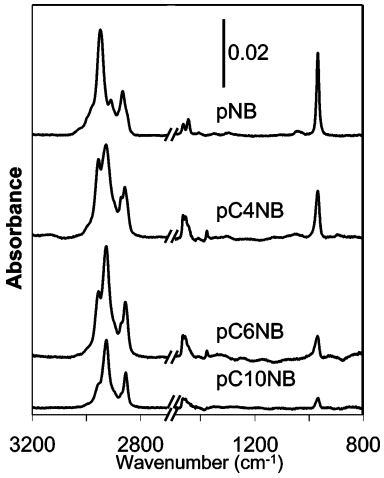


**Figure 3.** Reflectance−absorption infrared spectra of the indicated polymer films. The spectra have been offset vertically for clarity.

**Table 1. Relative Film Growth and Termination Rate Constants for Surface-Initiated Growth in Dichloromethane**

| monomer | $K$ (m $s^{-1}$) | $k_t$ ($s^{-1}$) |
|---|---|---|
| NB | $5.0 \times 10^{-8}$ | 0.0700 |
| C4NB | $5.0 \times 10^{-10}$ | 0.0013 |
| C6NB | $4.0 \times 10^{-10}$ | 0.0030 |
| C10NB | $5.3 \times 10^{-11}$ | 0.0025 |

where $k_p$ is the propagation rate constant and $k_t$ is an apparent, first-order termination rate constant, $M$ is the monomer concentration, $m_o$ is the mass of the monomer unit, $P_I$ is the initial concentration of propagating chains, and $\rho$ is the polymer density on the surface. Since $P_I$ is unknown for this series of monomers and highly challenging to determine for films initiated from 2-D surfaces, we combine $k_p$ and $P_I$ as a single rate term ($K$) for film growth

$$K = k_p P_I \quad (2)$$

that reflects both initiation and propagation and enables an overall comparison of film growth kinetics for this series of monomers. The resulting equation becomes

$$d = \frac{KMm_o}{k_t \rho}(1 - e^{-k_t t}) \quad (3)$$

We also estimate the density of the polymer on the surface from the density of the monomer (~0.865 g/$cm^3$), as similar to others.[27,33] The rate constants obtained from this analysis are used to assess the relative reactivity of the monomers studied.

Table 1 contains estimates of $K$ and $k_t$ based on fits of the kinetic results with eq 3. The rate constant for film growth ($K$) decreases with increasing length of the alkyl side chain, consistent with that found by Hatjopoulos and Register for the same monomers in solution using a Schrock-type catalyst.[23] Although Hatjopoulos and Register reported a 37% decrease in the rate of polymerization from NB to C10NB, our surface-initiated system exhibits a 3 order of magnitude decrease in $K$ over the same range of monomers. The contrast in the magnitude of change is not surprising due to the numerous differences (catalyst, cocatalyst, solvent, bulk vs surface) between the system reported by Hatjopoulos and Register and the surface-initiated system we employed, especially considering that $K$ here represents effects due to both initiation and propagation. The surface immobilization

(33) Yamamoto, S.; Ejaz, M.; Tsujii, Y.; Fukuda, T. *Macromolecules* **2000**, *33*, 5608−5612.

**Table 2. Peak Positions from RAIR Spectra**

| | wavenumber ($cm^{-1}$) | | | |
|---|---|---|---|---|
| mode | pNB | pC4NB | pC6NB | pC10NB |
| $\upsilon$-$CH_2$ cyclic | 2948 | 2955 | 2955 | 2955 |
| $\upsilon$-$CH_2$ cyclic | 2866 | 2871 | 2869 | 2871 |
| $\upsilon$-CH | 2911 | | | |
| $\upsilon_{as}$-$CH_2$ acyclic | | 2928 | 2927 | 2926 |
| $\upsilon_s$-$CH_2$ acyclic | | 2858 | 2856 | 2854 |
| $\delta$-$CH_2$ scissor | 1466/1447 | 1467 | 1467 | 1468 |
| $\delta$-C═CH | 968 | 968 | 969 | 969 |

of the catalyst will likely exaggerate the steric penalty associated with an alkyl substituent on the monomer over that of a solution polymerization. The choice of solvent also has a strong impact on film growth. Although a 1.0 M NB solution can grow films of comparable thickness solvated in both toluene (56 nm) and dichloromethane (78 nm), the thickness of a film grown from 1.0 M C4NB is ~35 times lower when grown in toluene (2 nm) versus dichloromethane (68 nm). Also shown in Table 1, the termination rate constant is reduced by a factor of 20−50 for *n*-alkylnorbornenes as compared with norbornene. The reduction is attributable to the alkyl side chain sterically hindering coupling and backbiting[27] (secondary-metathesis) based termination reactions.

**Influence of *n*-Alkyl Side Chains on Film Composition and Structure.** We used RAIRS to probe the composition and structure of the polynorbornene films. Control of the NB, C4NB, and C6NB monomer concentration allowed the growth of films of comparable thicknesses (~45 nm). The limited reactivity of the C10NB monomer prohibited the growth of 45 nm films; thus, ~8 nm pC10NB films are used for comparison. Figure 3 shows the relevant regions of representative RAIR spectra for all polymer films studied. The C−H stretching region of the RAIR spectra for polynorbornene consists of strong cyclic methylene stretching peaks ($\upsilon_{as}$ = ~2948 $cm^{-1}$, $\upsilon_s$ = ~2866 $cm^{-1}$) as well as a less intense tertiary C−H stretching peak at ~2911 $cm^{-1}$.[34] The position of the methylene scissoring peak at ~1450 $cm^{-1}$ is indicative of purely cyclic methylene functionality.[35] The olefin functionality is observed in the trans C═CH out of plane bending[34,35] peak (968 $cm^{-1}$) and the C═CH stretching peak (3030 $cm^{-1}$). Other groups have reported peak positions consistent with our observations.[4,34]

The addition of an *n*-alkyl side chain to the 5 position of the norbornene monomer alters the composition and structure of the resulting polymer. The polymer films with longer alkyl substituents exhibit increased *n*-alkyl functionality in the RAIR spectra with diminished polynorbornene functionality when compared to their shorter chained analogues. Specifically, the contribution of the acyclic methylene stretching ($\upsilon_{as}$ = 2926−2928 $cm^{-1}$, $\upsilon_s$ = 2854−2858 $cm^{-1}$) increases while the contributions of the cyclic methylene stretching ($\upsilon_{as}$ = 2948−2955 $cm^{-1}$, $\upsilon_s$ = 2866−2871 $cm^{-1}$) and the trans C═CH out of plane bending (968−969 $cm^{-1}$) decrease in an inversely proportional fashion. The shift of the methylene scissoring peak with the addition of the alkyl side chain is indicative of a deviation from a purely cyclic methylene component ($\delta$ $CH_2$ ~1447 $cm^{-1}$) toward a largely acyclic film ($\delta$ $CH_2$ ~1467 $cm^{-1}$).[35] The positions of the cyclic methylene stretching peaks in the poly(alkylnorbornene)s are shifted toward higher wavenumbers ($\upsilon_{as}$ = ~2955 $cm^{-1}$, $\upsilon_s$ = ~2870 $cm^{-1}$) indicative of a less crystalline conformation of the cyclopentane groups as compared to those in the original poly(norbornene) film.

Previous studies on polymethylene chains with highly crystalline chain packing exhibit asymmetric ($\upsilon_{as}$) and symmetric ($\upsilon_s$) methylene stretching at ~2918 and ~2850 $cm^{-1}$, respectively, whereas polymethylene chains in a liquid-like packing are shifted to higher wavenumbers. The poly(alkylnorbornene) films exhibit asymmetric and symmetric methylene stretching peaks at ~2926−2928 and ~2854−2858 $cm^{-1}$ (Table 2) indicative of liquid-like alkyl packing,[36] with incrementally more crystalline packing (lower wavenumber) as alkyl chain length is increased. We previously observed a comparable correlation in alkyl chain length with peak position in poly(hydroxyethyl methacrylate) films with *n*-alkyl side chains.[30] The greater van der Waals interactions between the longer *n*-alkyl chains likely drives the slight improvement in crystallinity in these polymers.[30]

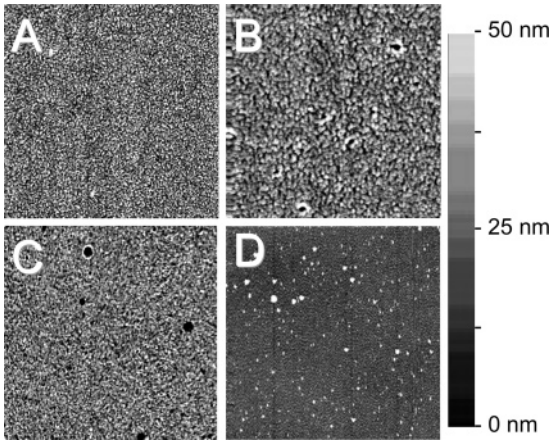


**Figure 4.** Atomic force microscopy images (25 $\mu$m × 25 $\mu$m) of pNB (A), pC4NB (B), pC6NB (C), and pC10NB (D) films.

Though the RAIR spectra demonstrate a slight increase in alkyl crystallinity in the poly(alkylnorbornene) films with increasing side-chain length, the crystallinity of the remainder of the film is likely hindered due to internal plasticization.[37] Hatjopoulos and Register have reported a $T_g$ decrease in bulk ROMP-type poly(alkylnorbornene)s with an increase in side-chain length, a strong indication that the structuring of the polymers and the analogous surface-initiated films is disrupted by moderate length alkyl chains.[23]

We used AFM to determine the morphology of the pNB and polyalkylnorbornene films. The surface-initiated polymerization of NB, C4NB, and C6NB generated a dense polymer coating (~45 nm) on the gold surface (Figure 4).[38] The small pinholes observed for the pC4NB and pC6NB are similar to much larger holes formed for pNB when NB was obtained from a different supplier (see the Supporting Information).[1] In contrast, the polymerization of C10NB resulted in the growth of polymeric islands on the gold surface. The ellipsometric film thickness for the pC10NB polymer layers (~8 nm) is used as a means to quantify the polymer on the surface and is not indicative of a true 8 nm film.

Contact angle goniometry is used to qualitatively access the composition and roughness of the surface of a film. Table 3 shows the advancing and receding water and hexadecane contact angles collected on all films studied. The advancing water contact angle for pNB ($\theta_A(H_2O)$ ~ 106°) is consistent with a predominant $CH_2$ surface and is similar to values of ~103° reported on polyethylene surfaces.[39] The contribution of the methyl terminus

(34) Planche, J. P.; Revillon, A.; Guyot, A. *J. Polym. Sci., Part A: Polym. Chem.* **1988**, *26*, 429−444.

(35) Silverstein, R.; Webster, F.; Kiemle, D. *Spectrometric Identification of Organic Compounds*, 7th ed.; John Wiley & Sons, Inc.: Hoboken, NJ, 2005.

(36) Berron, B.; Jennings, G. K. *Langmuir* **2006**, *22*, 7235−7240.

(37) Internal plasticization is a phenomenon where polymer side chains disrupt the overall polymer packing.

(38) AFM images obtained from different norbornene feedstocks are included in the Supporting Information.

**Table 3. Water and Hexadecane Advancing and Receding Contact Angles (deg) for Films on Gold**

| | water | | hexadecane | |
|---|---|---|---|---|
| film | $\theta_A$ | $\theta_R$ | $\theta_A$ | $\theta_R$ |
| pNB | $106 \pm 2$ | $81 \pm 3$ | <15 | <15 |
| pC4NB | $109 \pm 2$ | $83 \pm 4$ | $29 \pm 5$ | <15 |
| pC6NB | $114 \pm 2$ | $78 \pm 3$ | $23 \pm 5$ | <15 |
| pC10NB | $113 \pm 2$ | $81 \pm 1$ | <15 | <15 |

**Table 4. Film Capacitance, Resistance, and Ellipsometric Thickness Values for pNB and Poly(alkylnorbornene) Films**

| film | thickness (nm) | $\log(R_f)$ ($\Omega \cdot cm^2$) | $C_f$ ($nF/cm^2$) |
|---|---|---|---|
| vinyl linkage/catalyst | not measured | $1.3 \pm 0.1$ | $19000 \pm 1200$ |
| pNB | $49 \pm 2$ | $4.3 \pm 0.6$ | $250 \pm 170$ |
| pC4NB | $47 \pm 5$ | $4.5 \pm 0.5$ | $140 \pm 60$ |
| pC6NB | $42 \pm 7$ | $5.1 \pm 0.6$ | $150 \pm 50$ |
| pC10NB | $8 \pm 2$ | $2.2 \pm 0.2$ | $11000 \pm 4000$ |

on the alkyl chain causes an increase in hydrophobicity in the pC4NB, pC6NB, and pC10NB films ($\theta_A(H_2O) = 109-114°$), comparable to values obtained on pure methyl surfaces of SAMs ($\theta_A(H_2O) = 115°$).[40] The low surface tension of hexadecane amplifies surface energy differences in low-energy films and allows a more distinguishing measure of the surface properties of low-energy films via contact angle goniometry. The predominant $CH_2$ surface of the pNB film allows the wetting of the surface by hexadecane ($\theta_A(HD) < 15°$). The methyl functionality of the pC4NB films causes an increase in the hexadecane contact angle to 29°. Interestingly, the hexadecane contact angle decreases as the length of the alkyl side chain increases to that of a pC6NB ($\theta_A(HD) = 23°$) and a pC10NB film ($\theta_A(HD) < 15°$). The additional length of the alkyl side chain of the polymer dilutes the methyl functionality, which is responsible for the oleophobicity of the film. In the case of pC10NB, the cluster-like morphology (see Figure 4D) leads to a lower hexadecane and higher water contact angles, as predicted by the effect of roughness on contact angles.[2,41,42]

**Barrier Properties.** We used electrochemical impedance spectroscopy to investigate the barrier properties of the surface-initiated poly(alkylnorbornene) films in the presence of $K_3Fe(CN)_6$ and $K_4Fe(CN)_6$ in 0.1 M $NaSO_4$(aq). Representative Bode plots for ~45 nm films of pNB, pC4NB, and pC6NB are shown in Figure 5. Due to the limited reactivity of the C10NB monomer, an ~8 nm pC10NB film is used. The impedance spectra of the polymer films are best fit with a Randle's equivalent circuit[43] modified with a Warburg impedance term to account for a resistance to mass transfer.[44] Table 4 shows film thicknesses along with the resistance ($R_f$) of the films against penetration by redox probes, and capacitance ($C_f$) values. Good barrier films typically exhibit high resistance and low capacitance values.[2,30-32,44] The film resistances ($R_f \sim 10^5$ $\Omega \cdot cm^2$) and capacitances (~200 nF) of the pNB, pC4NB, and pC6NB films are comparable to that of other hydrocarbon surface-initiated films with a pronounced increase in film resistance as the chain length of the hydrophobic alkyl group is increased.[30] When compared to pNB, the increase in resistance due to the added hydrophobicity for the pC4NB and pC6NB appears to outweigh the greater density

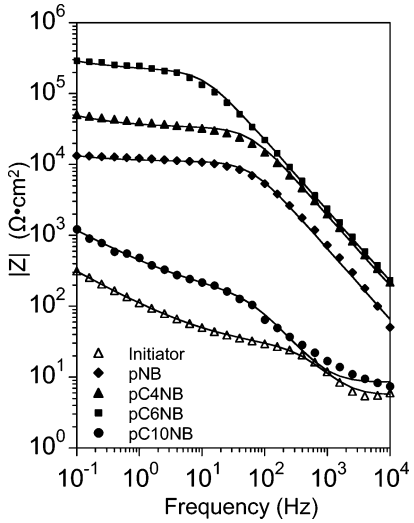


**Figure 5.** Electrochemical impedance spectra obtained in 1 mM $K_3Fe(CN)_6$ and 1 mM $K_4Fe(CN)_6$ in 0.1 M $Na_2SO_4$(aq) for the indicated films on gold. Solid curves represent fits of the data using appropriate equivalent circuit models.

of pinholes in these films (Figure 4). The low film resistance ($R_f \sim 10^2$ $\Omega \cdot cm^2$) and high capacitance ($C_f \sim 11$ $\mu F$) of the pC10NB films are attributed to the nonuniform, cluster-like film growth as shown in Figure 4D.

## Conclusions

The preparation of surface-initiated ROMP-type poly(*n*-alkylnorbornene) films is easily achieved through three sequential and rapid reactions, including assembly of allyl mercaptan, catalyst attachment, and polymerization. Polymerization of butylnorbornene and hexylnorbornene yields dense films with liquid-like packing of the alkyl side chains, whereas decylnorbornene polymerizes into discrete clusters. Increasing the length of the alkyl side chain on the monomer decreases the rate of film growth and limits the ultimate thickness of the polymer film. The methyl terminus of the alkyl side chains decreases the surface energy beyond that of a typical polynorbornene film. The added hydrophobicity of pC4NB and pC6NB correlates with an enhanced resistance against redox probes as compared with pNB films, whereas barrier properties of the pC10NB are consistent with a poor coverage of the metallic substrate. These films contain internal olefin groups to enable further reactive processing and tailorability of film and surface properties, which we will highlight in a subsequent report.

**Acknowledgment.** The project was supported by the U.S. Department of Energy (ER46239). The authors thank Dr. Ed Elce (Promerus Electronic Materials) for generously providing the alkylnorbornene monomers. We thank Dr. SonBinh T. Nguyen at Northwestern University for helpful discussions on ROMP. We also thank Christina Payne for her AFM data conversion software. B.J.B. thanks the Vanderbilt Institute of Nanoscale Science and Engineering for a fellowship. We thank Professor Bridget Rogers for the use of the ellipsometer.

**Supporting Information Available:** Comparison and discussion of polynorbornene films grown using norbornene from two commercial sources. This material is available free of charge via the Internet at http://pubs.acs.org.

LA7017902

(39) Holmes-Farley, S. R.; Reamey, R. H.; McCarthy, T. J.; Deutch, J.; Whitesides, G. M. *Langmuir* **1985**, *1*, 725−740.
(40) Laibinis, P. E.; Whitesides, G. M.; Allara, D. L.; Tao, Y. T.; Parikh, A. N.; Nuzzo, R. G. *J. Am. Chem. Soc.* **1991**, *113*, 7152−7167.
(41) Wenzel, R. W. *Ind. Eng. Chem.* **1936**, *28*, 988−994.
(42) Sun, T. L.; Wang, G. J.; Feng, L.; Liu, B. Q.; Ma, Y. M.; Jiang, L.; Zhu, D. B. *Angew. Chem., Int. Ed.* **2004**, *43*, 357−360.
(43) Jennings, G. K.; Laibinis, P. E. *J. Am. Chem. Soc.* **1997**, *119*, 5208−5214.
(44) Brantley, E. L.; Jennings, G. K. *Macromolecules* **2004**, *37*, 1476−1483.